Representation Error of Oceanic Observations for Data Assimilation

PETER R. OKE AND PAVEL SAKOV

CSIRO Marine and Atmospheric Research, and Wealth from Oceans Flagship Program, Hobart, Tasmania, Australia

(Manuscript received 14 February 2007, in final form 10 September 2007)

ABSTRACT

A simple approach to the estimation of representation error (RE) of sea level (η), temperature (T), and salinity (S) observations for ocean data assimilation is described. It is assumed that the main source of RE is due to unresolved processes and scales in the model. Therefore, RE is calculated as a function of model resolution. The methods described here exploit the availability of mapped sea level anomalies (mSLAs) and along-track sea level anomalies (atSLAs). The mSLA fields or atSLA observations are regarded as the true ocean state. Here, they are averaged according to the resolution of the model grid, and the averaged field is taken as a representation of the true state on the given grid. The difference between the original data and the averaged field is then regarded as the RE for η. Subsequently, the RE is projected for η over depth using a standard technique, giving an estimate of the RE for T and S. Examples of RE estimates for an intermediate- and high-resolution global grid are presented. It is found that there is significant spatial variability in the RE for η, T, and S, with values that are typically greater than or comparable to measurement error, particularly in regions of strong mesoscale variability.

1. Introduction

Estimation of both background and observation errors is critical for optimal data assimilation. Data assimilation typically involves the calculation of an analyzed state vector $\mathbf{w}^a$, by combining a background field $\mathbf{w}$ and a vector of observations $\mathbf{d}$. The influence of the observations on the analysis depends on estimates of the background and observation error covariances that are quantified by the matrices $\mathbf{P}$ and $\mathbf{R}$, respectively. Many data assimilation methods seek to minimize the error variance of the analysis. Kalman filter–based algorithms express the optimal solution as

$$\mathbf{w}^a = \mathbf{w} + \mathbf{PH}^{\mathrm{T}}(\mathbf{HPH}^{\mathrm{T}} + \mathbf{R})^{-1}(\mathbf{d} - \mathbf{Hw}), \qquad (1)$$

where $\mathbf{H}$ is the observation operator that interpolates from model to observation space. A very simplistic interpretation of data assimilation is that it is an exercise in curve fitting. For ensemble, Kalman filter–based algorithms, such as ensemble perturbations, are fitted to background innovations (model–observation differences). With this interpretation in mind, the diagonal elements of $\mathbf{P}$ and $\mathbf{R}$ provide error bars that guide the degree to which the innovations are fitted. Clearly, the correct estimates for both $\mathbf{P}$ and $\mathbf{R}$ are critically important for any application of data assimilation (Houtekamer and Mitchell 2005).

There is a vast literature on methods for estimating the background error covariances that are quantified by $\mathbf{P}$ (e.g., Ngodock et al. 2006, and references therein). Background errors include errors in initial and boundary conditions as well as model errors (e.g., Daley 1992; Mitchell and Houtekamer 2000). Observation errors, quantified by $\mathbf{R}$, include measurement errors and representation errors (REs; Daley 1993), which are often called representativeness errors (e.g., Janic and Cohn 2006). This paper is concerned with the estimation of RE.

It is widely acknowledged in the data assimilation community that RE is the component of observation error due to unresolved scales (e.g., Thacker 2003; Janic and Cohn 2006; Leeuwenburgh 2007; Kohl et al. 2007), or misspecification of the observation operator $\mathbf{H}$ (Liu and Rabier 2002). More generally, RE could be attributed to any physical processes appearing in the observations but not in the model (Anderson et al. 2005; Ponte et al. 2007; Zaron and Egbert 2006). RE has also been referred to as forward interpolation error (Lorenc 1986; Daley 1993), which is subject to the effects of

Corresponding author address: Peter R. Oke, CSIRO Marine and Atmospheric Research and Wealth from Oceans Flagship Program, Hobart, Tasmania, Australia.
E-mail: peter.oke@csiro.au

DOI: 10.1175/2007JTECHO558.1

discretization error and limited resolution (Mitchell and Daley 1997). RE is acknowledged as being dependent on the resolution of the model grid (Mitchell and Daley 1997; Desroziers et al. 2001; Cummings 2005). Indeed, Janic and Cohn (2006) demonstrate that RE is also state dependent and correlated in time.

To understand the need for RE, consider a case in which a single point observation is available. Suppose the observation is perfect, with no measurement error, and suppose that it is to be assimilated into a model that only represents large-scale circulation. This observation represents spatial and temporal scales as well as physical processes that are not represented by the model. In this case, the observation contains RE. Consequently, the model should not be tightly constrained to this observation. Lorenc (1986) suggests that the RE is justified by redefining *truth* to contain only those scales that we wish to analyze. In practice, this is accommodated for in data assimilation by including an estimate of the variance of RE in $\mathbf{R}$. Clearly, for data assimilation, we do not wish to analyze subgrid-scale features. Quantifying this component of RE, for inclusion in $\mathbf{R}$, therefore requires us to quantify the variance of the subgrid-scale features. The development of a practical approach to this task is the goal of this study.

It is important to recognize the difference between RE and model error in the context of data assimilation. In contrast to RE, model error can result from imperfect parameterizations, numerical approximations, inaccurate fluxes, and so on. Not only do RE and model error have distinctly different meanings but they are also treated differently in data assimilation. Specifically, RE is added to the observation error estimates (Lorenc 1986). That is, RE increases $\mathbf{R}$ in (1), and this results in analyses that do not fit the observations as closely. By contrast, model error is accommodated for by inflating the estimates for the background error variance (e.g., Daley 1992; Mitchell and Houtekamer 2000; Bishop et al. 2001; Evensen 2003). That is, model error increases $\mathbf{P}$ in (1), which results in analyses that fit the observations more closely. Importantly, Lorenc (1986) notes that only scales resolved by the model basis should be included in the background-error covariance matrix $\mathbf{P}$.

While all data assimilation applications include some estimate of the RE in $\mathbf{R}$, there is a wide range of approaches used. Here, we provide a sample of various approaches taken from oceanographic examples. Most applications assume that RE is stationary in time. In some cases, a spatially uniform inflation to $\mathbf{R}$ is used (e.g., Rogel et al. 2005; Oke et al. 2005). In other cases, a nonuniform inflation to $\mathbf{R}$ is applied, depending on the expected level of eddy activity in different regions (e.g., Derber and Rosati 1989; Oke et al. 2008; Schiller et al. 2008). Some applications assume that RE is proportional to the variance of observations (Kohl et al. 2007). There are many cases in which RE for potential temperature (T) and salinity (S) is assumed to be horizontally uniform and depth dependent (e.g., Stammer et al. 2002; Brasseur et al. 2006). Cummings (2005) is a notable exception, because he uses a state-dependent estimate for RE in which the uncertainty in physical processes, such as internal waves, is parameterized.

The literature describes several systematic methods for estimating RE. Some studies have investigated how RE should be treated in data assimilation for various idealized cases (e.g., Liu and Rabier 2002; Janic and Cohn 2006). A more practical example is described by Richman et al. (2005), in which a systematic approach for estimating RE for SST, appropriate for coarse-resolution models, is presented. Etherton and Bishop (2004) and Ponte et al. (2007) provide model-based estimates of RE utilizing the differences between two models of different resolution. These approaches have some very nice properties; however, for many researchers, the overhead in configuring, tuning, and integrating a high-resolution model for the purpose of estimating RE is prohibitive and therefore impractical. In this paper, we describe an efficient method that uses either mapped sea level anomalies (mSLAs) or along-track sea level anomalies (atSLAs) as well as vertical projection techniques to provide consistent estimates of RE for η, T, and S.

This paper is organized as follows: an mSLA-based method and an atSLA-based method for estimating the RE for η, T, and S are described in section 2. Section 3 shows a series of applications, along with a demonstration of the impact that different estimates for RE can have on analysis increments for a realistic application. A discussion is presented in section 4, followed by our conclusions in section 5.

2. Method

As stated above, RE is the component of observation error due to unresolved scales and processes. In this paper, we assume that the main source of RE is due to limited resolution. Estimation of RE therefore requires us to quantify the variance of the subgrid-scale features. This is the goal of the methods described below. We present the details of these methods with explicit reference to oceanographic applications, but note that they can easily be generalized to other geophysical applications in which mapped, modeled, or well-resolved observed fields are available.

We describe two very similar methods to estimate RE. Both methods make use of either mSLA fields or atSLA observations. In each case, these data are supposed to represent the real world. We simply compute spatial averages of these fields to eliminate subgrid-scale features, and we regard this averaged field as an estimate of the *redefined truth* that is compatible with the model grid (Lorenc 1986). The differences between the original fields and the averaged fields therefore provide an estimate of the RE.

a. mSLA-based method

Satellite altimetry is currently the best-resolved ocean observing system available for measuring mesoscale variability (Pascual et al. 2006) and is likely to remain so in the foreseeable future. The mSLA-based method involves the use of mSLA fields that are based on altimetric observations that have an along-track resolution of approximately 7 km and a temporal resolution of 10 days. Here, we use weekly maps of mSLA that are produced by Archiving, Validation, and Interpretation of Satellite Oceanographic data (AVISO) and are generated by combining atSLA observations from all altimetric missions using optimal interpolation (OI). The details of the OI mapping are described by Ducet et al. (2000). Briefly, the length scales used for the OI range from 100 km in the zonal and meridional directions at 60°N–S, to 250 (350) km in the meridional (zonal) direction at the equator. Maps are produced on a global 1/3° Mercator grid with 18.5-km resolution at 60°N–S and 37-km resolution at the equator.

Estimation of the RE for η using the mSLA fields involves a number of assumptions. Specifically, we assume that the mSLA fields are available on a grid that has a higher resolution than the model. This method is therefore only appropriate for application to intermediate- to coarse-resolution grids (i.e., 1° resolution or coarser; for higher-resolution grids, see the atSLA-based method described below).

It is also assumed that the mSLA fields resolve all scales of variability. It is known that oceanic features on sub-1/3° scales do exist. The validity of our results using this method is therefore based on an implicit assumption that *most* of the variability is resolved by the mSLA fields. This assumption is not valid everywhere: for example, in the equatorial region where Legeckis waves and their associated fronts are not resolved, and where eddies that are smaller than the length scales used in the OI mapping occur. These assumptions will result in estimates for RE that are probably too small.

The mSLA-based method involves the computation of RE for η in three simple steps. An example of each step is shown in Fig. 1 for a 1° grid in the North Atlantic Ocean. The steps are as follows:

1) For a given time period, we take an mSLA field (e.g., Fig. 1a) that is here regarded as the best available estimate of the real world and calculate the best possible estimate that a model could produce by averaging the mSLA field on the model grid, by applying a simple boxcar filter. This field is referred to here as the *averaged mSLA field*, an example of which is shown in Fig. 1b. For this example, there is a rich eddy field along the path of the Gulf Stream extension in the mSLA map (Fig. 1a). When averaged onto the 1° grid, some of the details of the eddy field are lost, and only the broad scales and large eddies are retained (Fig. 1b).
2) Calculate the averaged and *interpolated mSLA* field by interpolating the averaged mSLA field back to the 1/3° grid using the operator $\mathbf{H}$ (Fig. 1c). This field can be considered a redefined truth that contains only those scales we wish to analyze (Lorenc 1986).
3) Calculate the difference between the original mSLA field (Fig. 1a) and the redefined truth (Fig. 1c), the result of which can be regarded as an estimate of the RE for this point in time (Fig. 1d). For this example, the RE field resembles the original eddy field but with shorter length scales.

For a model grid that is coarser than the mSLA grid, the RE necessarily has scales that are finer than the grid spacings of the model grid. The averaged mSLA field in each grid cell (Fig. 1b) is a better representation of the value at the cell center compared to the cell boundaries that lie between each grid point. This subtlety is evident in Fig. 1d, where there are typically local minima at cell centers and local maxima at cell corners. This indicates that an observation in the center of a grid cell, near the grid points, has smaller RE than an observation near the boundary of grid cells between grid points.

b. atSLA-based method

An obvious limitation of the mSLA-based method, described above, is that the mSLA fields do not resolve all scales of variability; in addition, the method is not applicable for grids with resolutions that are close to or higher than those of the mapped product (here, 1/3°). We therefore present an alternative method that uses the atSLA observations to estimate the RE for η in three simple steps. An example of each step is shown in Fig. 2 for a 1° grid in a small region of the Gulf Stream extension in the North Atlantic Ocean. These steps are as follows:

1) For a given time window (here, a 7-day period), identify all atSLA observations that fall within each grid cell and calculate the average (Fig. 2a). Pro-

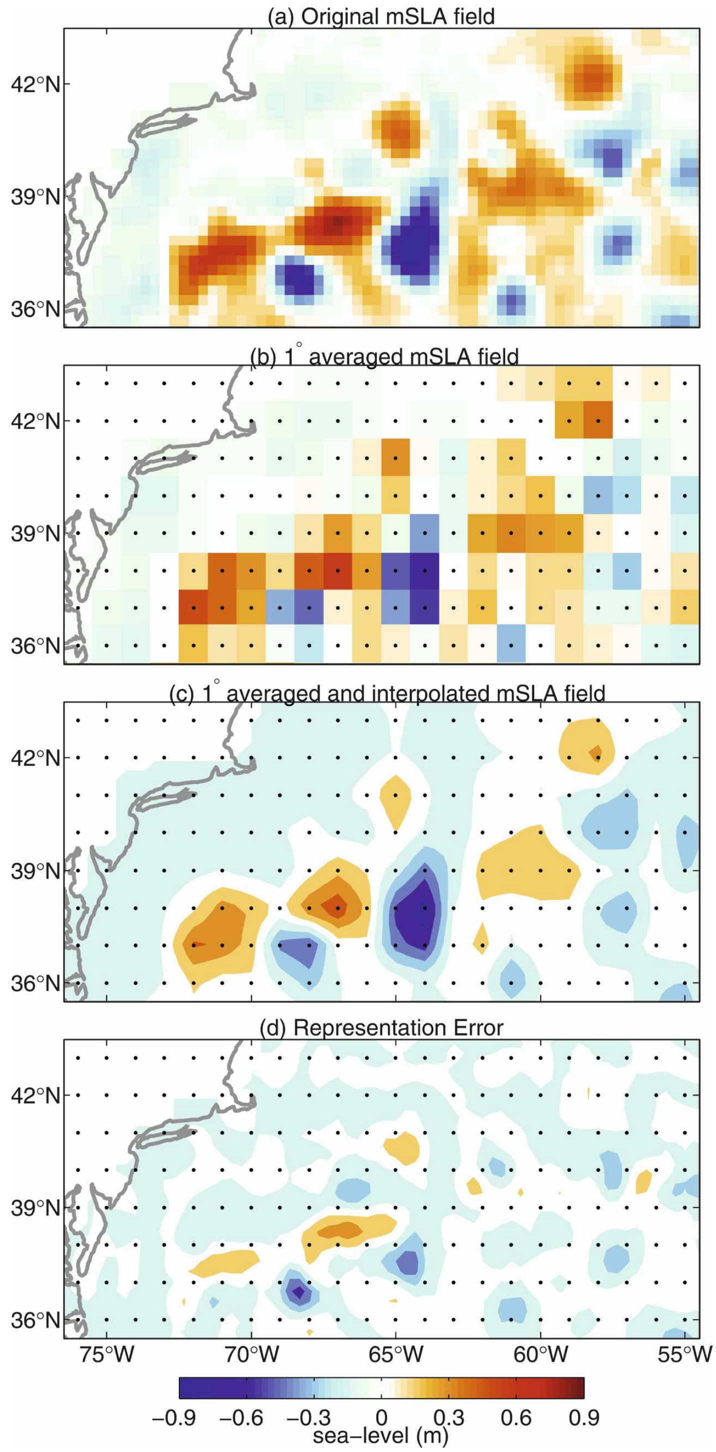

FIG. 1. Example of each step of the calculation of the RE for η, showing the (a) orginal mSLA field, (b) 1° averaged mSLA field, (c) 1° averaged and interpolated mSLA field, and (d) the difference between (a) and (c), thus providing an estimate of the RE for η. The grid points are plotted in (b)–(d).

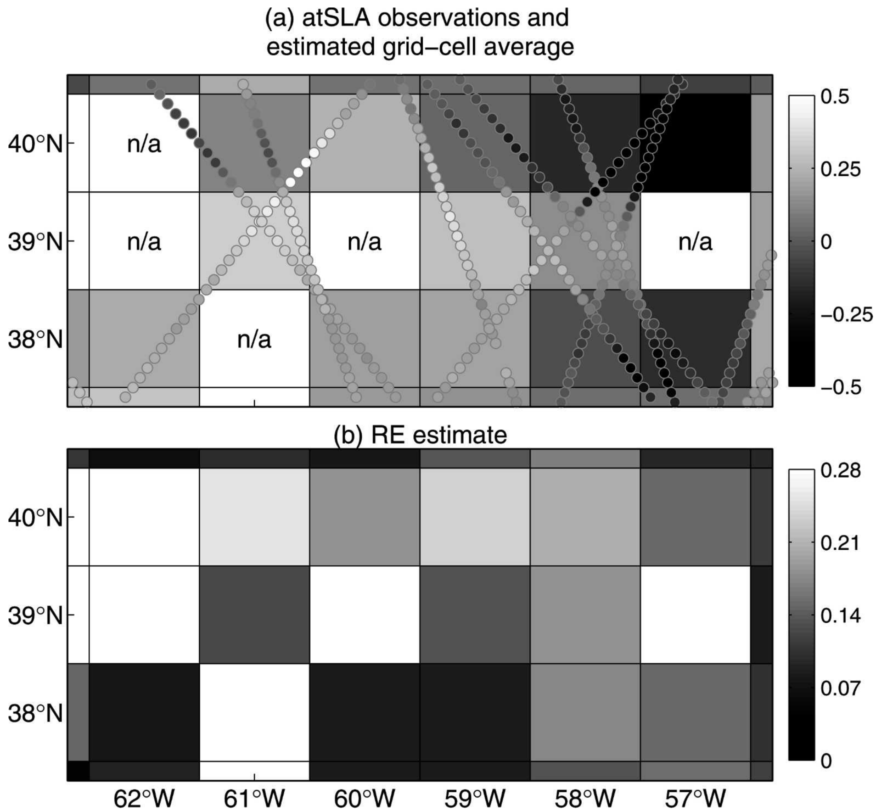

FIG. 2. Example of each step of the atSLA-based method for estimating RE for η, showing (a) atSLA observations (colored circles, showing every second; the truth) and the grid-cell average (the best-possible model estimate), and (b) the std dev of the difference between the truth and the best-possible model estimate for each grid cell, providing an estimate of the RE for η.

vided that there are enough raw atSLA observations in the grid cell and that the observations adequately span the grid cell, this can be regarded as the redefined truth that contains only those scales we wish to analyze (Lorenc 1986).

2) Compute the difference between the raw atSLA observations and the cell average calculated above. These values can be regarded as estimates of the RE for this particular point in time for this grid cell.
3) Provided there are enough atSLA observations in the grid cell, calculate the standard deviation of the differences from above. This provides an estimate for the cell-averaged RE for η for this particular point in time for this grid cell.

Another simple demonstration of the atSLA-based approach is shown in Fig. 3. This example shows atSLA observations along a single altimeter track that runs through the Tasman Sea. It exhibits eddy-scale features that are not well represented on a 1° grid. In the context of this example, the 1° boxcar-averaged field represents a redefined truth that contains only those scales we wish to analyze (Lorenc 1986). Also shown in Fig. 3b is the RE estimate that corresponds to the atSLA fields. This is simply the standard deviation of the differences in each grid cell between the atSLA observations and the cell-averaged fields. Clearly, the RE estimates presented here suffer from sampling error. The impact of sampling error is reduced when more observations are included in this analysis, as presented in Fig. 2.

c. *Consistent RE estimates for T and S*

Estimates of the RE for T and S are readily produced by projecting the RE estimates for η from the weekly fields vertically over depth. There are many techniques available for estimating T and S profiles based on sea level anomalies (SLAs). These include the use of observation-derived regressions (Ridgway et al. 2002), gravest empirical modes (Perez-Brunius et al. 2004), and the scheme of Cooper and Haines (1996, hereafter CH96), of which there are many variants (e.g., Troccoli and Haines 1999). The details of the method for projecting RE for η to RE for T and S are not the focus of

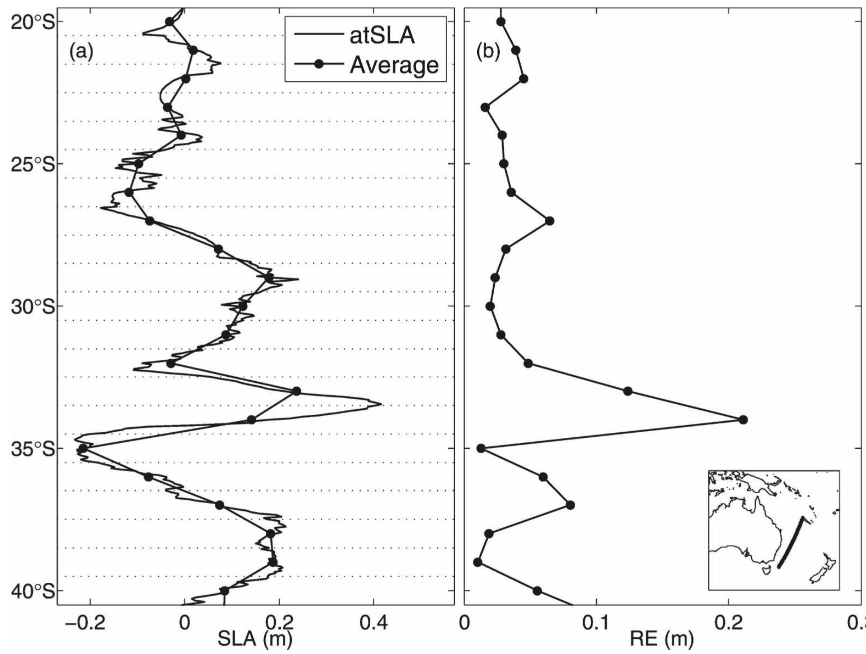

FIG. 3. An example of (a) atSLA observations and (b) 1° averages along a track that runs through the Tasman Sea (inset) the corresponding estimate of RE for η.

this paper. We therefore employ the most widely used and easily implemented of these techniques, namely, the CH96 scheme, which assumes that variations in sea level are not barotropic and are mainly related to the vertical excursion of T and S profiles. Although this may generally be true in the low- to midlatitudes, it is unlikely to be true at high latitudes (e.g., in the Southern Ocean). Given an SLA and an underlying T and S profile, implementation of CH96 involves a vertical shift, or heave, of the water column so that the influence of the SLA on bottom pressure is reduced to zero. Generally, a positive (negative) anomaly in η corresponds to a deepening (shoaling) of isopycnals. Therefore, an anomaly in η is converted to an anomaly in T and S in the underlying water column. This scheme has a number of nice properties and has been used successfully in many studies for the assimilation of altimetric observations (e.g., Fox et al. 2000).

3. Results

a. *Coarse-resolution application*

The calculations described in section 2 are repeated here for a global 1° grid using weekly mSLA fields and weekly 7-day batches of atSLA observations for the time period 1993–2005. A demonstration of the significant temporal and spatial variability of atSLA-based RE estimates in regions of energetic eddy activity is shown in Fig. 4. This figure shows longitude time plots of RE for a section in the North Atlantic Ocean in the region of the Gulf Stream extension and a section in the Tasman Sea. Time-varying estimates of RE, such as those plotted in Fig. 4, could be included directly in $\mathbf{R}$. Indeed, such estimates could be computed online, as part of the data assimilation scheme. Clearly, the estimates in Fig. 4 are noisy and are likely to suffer from sampling error, depending on factors such as the spatiotemporal positions of satellite tracks, the number of altimeter missions, and the details of the spatial averaging.

An alternative to using time-varying estimates of RE (Figs. 4b,d) is to compute a stationary field, such as the time averages shown in Figs. 4a,c. Clearly, the temporal variability in RE means that a time average will sometimes underestimate and sometimes overestimate the true RE. This may lead to underfitting, in which useful information is discarded, and overfitting, in which noise is introduced into an analysis. As a consequence, the data assimilation scheme will be less optimal. The problem of overfitting is probably most serious because it can degrade the model solution and even cause the model to become numerically unstable. There are many options to avoid overfitting; for example, a stationary estimate based on the 90th percentile could be used as a somewhat conservative approach. For every data as-

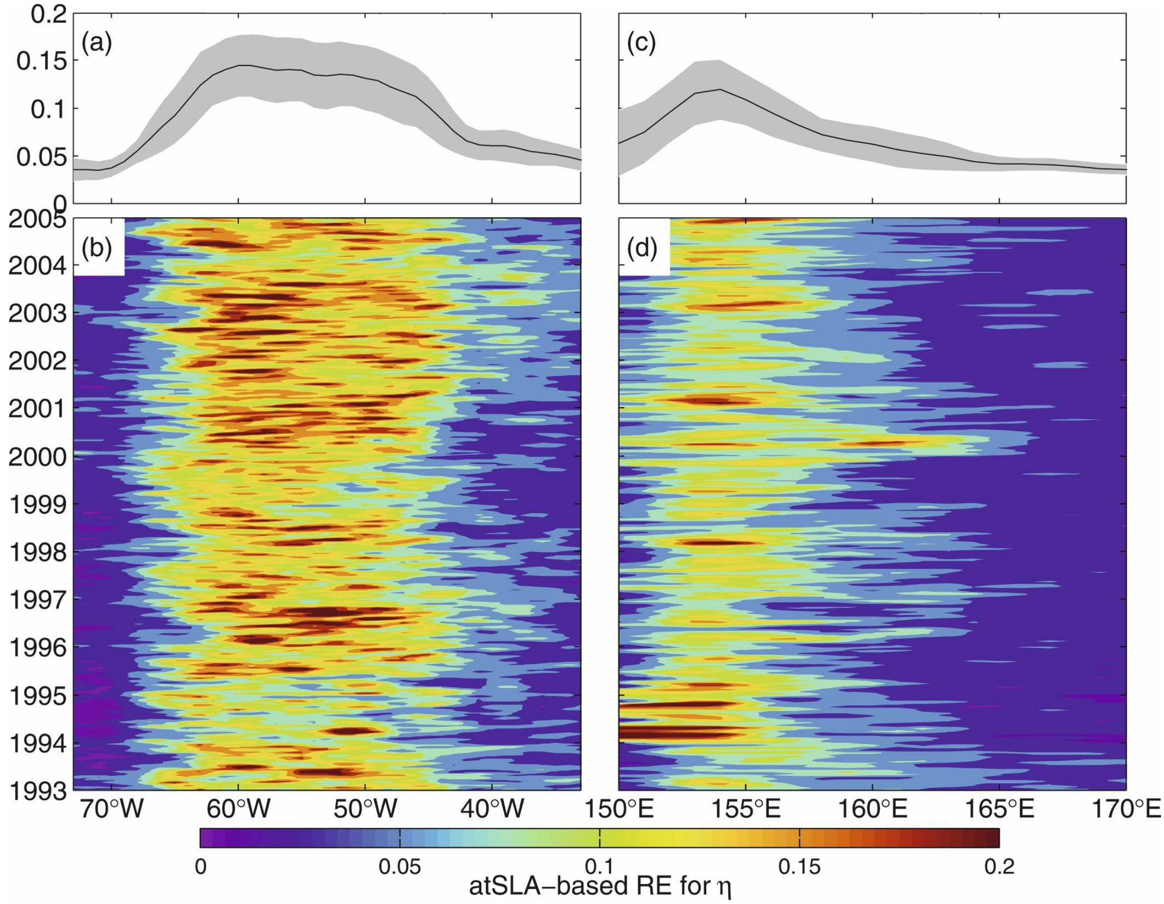

FIG. 4. A demonstration of the temporal and spatial variability of atSLA-based RE estimates in regions with energetic eddy activity, showing (a), (c) time average and std devs (gray) and (b), (d) time series of the estimated RE for η along a longitude section in the (left) North Atlantic Ocean at 40°N and in the (right) Tasman Sea at 25°S. RE estimates are based on atSLA observations and are computed for a 1° grid.

similation application, this aspect of the assimilation requires tuning, probably by trial and error. Our aim here is not to provide a fail-proof method for estimating RE but instead to describe a general approach that might lead to improved estimates of RE, and thereby lead to more optimal data assimilation. In the remainder of this paper, for simplicity, we restrict our attention to time averages or root-mean-square (RMS) estimates of RE.

Stationary estimates of the RE for η are presented using the mSLA- and atSLA-based methods described above for a global 1° grid (Fig. 5). Included in Fig. 5 is the RMS mSLA-based estimate (on the 1/3° mSLA grid; Fig. 5a), a grid-cell-averaged version of the mSLA-based estimate (on the model grid; Fig. 5b), and a time average of the atSLA-based estimate (Fig. 5c). We include the grid-cell-averaged mSLA-based estimate (Fig. 5b) so it can be directly compared to the atSLA-based estimate, both of which are on the model grid. Comparison of the grid-cell-averaged estimates (Figs. 5b,c) shows good qualitative agreement, with the largest RE in the boundary currents and along the path of the Antarctic Circumpolar Current (ACC). We also note that these estimates are in good qualitative agreement with the estimates provided by Ponte et al. (2007) using a model-based method.

We note that the detailed subgrid-scale structure evident in Fig. 1d is also evident in the variance fields in Fig. 5a. For this example, RE for the cell centers is typically about 30% smaller than the RE for cell corners.

Both methods considered here indicate that the RE for η is smallest in the tropics and away from the boundary currents. The mSLA-based estimates suggest that the RE in these regions is close to zero, while the atSLA-based estimates suggest that the RE is between 3 and 5 cm. The difference between the atSLA- and mSLA-based estimates is presented in Fig. 5d. This

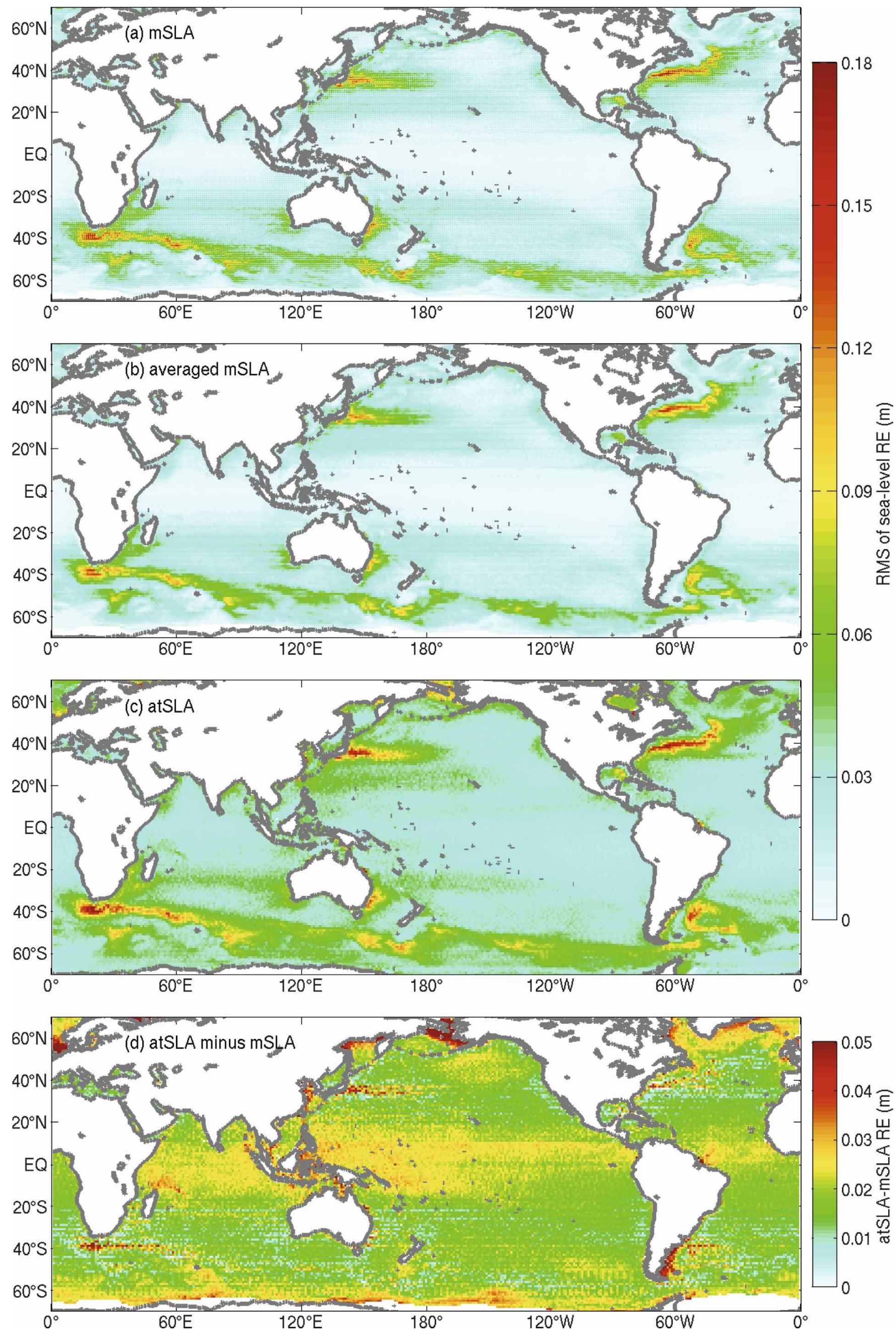

FIG. 5. RMS and time-average estimates of the RE for η on a 1° global grid using (a) the mSLA-based method, (b) the grid-cell average of (a), (c) the atSLA-based method, and (d) the difference between the RE estimates using the atSLA and the mSLA fields. All fields are computed using mSLA fields and atSLA observations for the period 1993–2005.

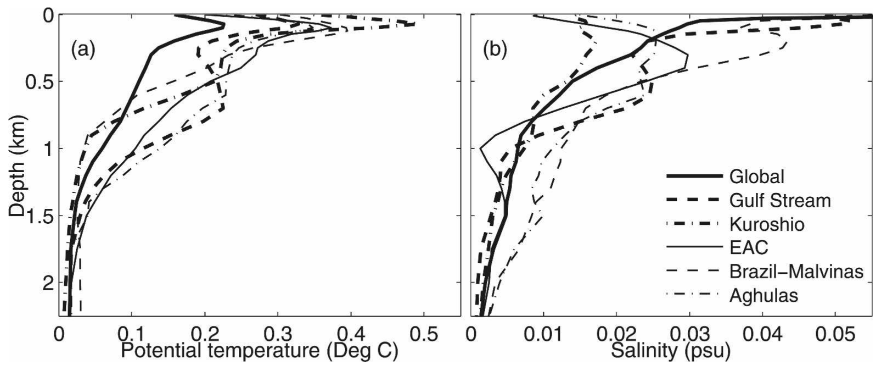

FIG. 6. RMS of the RE for (a) T and (b) S for a 1° grid for the entire globe and the major western boundary current regions using the mSLA-based estimates of the RE for η and CH96.

shows that there are regions where these two estimates are quite different; in most of the western boundary currents, the Gulf Stream and Kuroshio extensions, and the Aghulas retroflection region, the atSLA-based estimates are more than 5 cm larger than the mSLA-based estimates. There are also differences off Antarctica, where the atSLA approach probably suffers from sampling error, and in the tropics, where the long length scales in the OI mapping of the mSLA (Ducet et al. 2000) are likely to exclude more small-scale variability. Some of these differences may also be attributed to aliasing from the time window used by AVISO in the OI (Ducet et al. 2000). We might reasonably expect these differences to be greater than the measurement errors of the altimeters, which are 2–4 cm (Ducet et al. 2000). Given these limitations, the RE estimates from mSLA and atSLA are generally in good agreement.

We generally regard the mSLA-based estimates to be too small, because the assumption that the mSLA fields represent all spatial scales is clearly flawed. As noted above, the mSLA fields do not properly represent the mesoscale field with scales that are smaller than the length scales used in the OI mapping. By contrast, we generally regard the atSLA-based estimates to be too large. This is because the limited coverage of altimetry results in a sampling error, which tends to inflate the RE estimates, and because of the treatment of atSLA observations in 7-day batches. With regard to the sampling error, for some individual estimates of RE from atSLA observations, there may be only a few observations in each grid cell (see Fig. 2). The resulting RE estimate is therefore likely to be somewhat noisy and unreliable. We have attempted to eliminate the negative effects of this sampling error by only including RE estimates when there are more than 10 atSLA observations available in a grid cell. Moreover, an estimate of the variance, or RMS, of the RE for a grid cell is only computed if there are more than 50 estimates of RE for the period 1993–2005. Admittedly, these criteria have no sound basis. As a result of this processing, some grid cells do not have a valid estimate of the RMS fields for Fig. 5, in which case we simply interpolate from adjacent cells to obtain a complete field. Another source of error that results in the atSLA-based estimates being too large is the treatment of observations in 7-day batches. Recall from section 2b that we identify all atSLA observations in a grid cell from a 7-day time window. We subsequently regard the average of these observations to be an estimate of the redefined truth, which contains only those scales we wish to analyze (Lorenc 1986), and therefore any deviation from this average is regarded as an error. Clearly, some of the deviations from the batch averages are not errors attributable to RE but are part of the short time-scale signal that can be resolved by the model. This assumption therefore results in an overestimate of the RE.

In addition to estimates of RE for η, it is typically necessary to estimate RE for T and S, where hydrographic observations are to be assimilated. The CH96 scheme is applied here to convert weekly estimates of RE for η using the mSLA-based method for the 1° grid into estimates of RE for T and S. This requires some background estimate of the T and S fields. We use a 1/2°-resolution global climatology: a blend of Ridgway et al. (2002) and Levitus and Boyer (1994). We compute weekly estimates of the RE for T and S for the 1° grid for the period 1993–2005. Plots of the global-averaged profiles of the RMS of the estimated RE for T and S are shown in Fig. 6, along with averaged profiles for the major boundary currents. Notably, the profiles in different boundary currents are very different. This highlights the errors introduced by assuming that RE can be calculated from a single profile for T and S.

Clearly, the climatological T and S fields used to compute the estimates in Fig. 6 are not generally valid. As a result, these RE estimates contain error, as does any stationary estimate, as discussed above. As an alternative, state-dependent estimates of the RE for T and S could be obtained using the time-dependent estimates of RE for η and the CH96 scheme using the model T and S fields. This represents a considerable computational overhead that may be impractical. A more computationally efficient approach could be the use of the RMS of the heave field, denoted here as σ^{heave}.

Although this field is based on the climatological T and S fields referred to above, it may be a reasonable approximation to the statistics of the heave at any time. A state-dependent approximate RE for T and S, $\sigma_{\text{RE}}^{T,S}$, could be efficiently obtained by

$$\sigma_{\text{RE}}^{T,S} = \sigma^{\text{heave}} \frac{\partial(T, S)}{\partial z}, \tag{2}$$

where z is the depth. This formulation provides an approximation to the RE for T and S that reflects the local and time-varying stratification. In practice, the gradient term $\partial(T, S)/\partial z$ can be derived either from the model background state or from an observed profile.

b. *High-resolution application*

One of the advantages of the atSLA-based method is that it can readily be applied to high-resolution applications. As an example of such an application, the RMS of RE for η is shown for a 1/3° global grid in Fig. 7. This field indicates that the RE for η is quite large in the boundary currents, with values of 6–10 cm, and it is also large along the path of the ACC, with values of 5–6 cm. Even in the tropics and the relatively quiescent regions of the ocean basins, the RE for η remains at a level comparable to the expected measurement error of altimetry. Figure 7b shows the RE in the North Atlantic Ocean. This figure highlights the inhomogeneity of the RE for η, with large values in the Gulf Stream and its extension, and large values in the region of the Loop Current in the Gulf of Mexico. In practice, use of the RE estimates in Fig. 7 for data assimilation will require a complete field of RE, without the missing values evident here. We suggest that the calculated field could easily be mapped onto the full model grid to facilitate easy use.

c. *Sensitivity of analysis increments to RE estimates*

To demonstrate the impact of different estimates for RE on an analysis produced by a data assimilation system, we present results from an application using an ensemble optimal interpolation system applied to a global ocean model that has a variable resolution. Specifically, we use the Bluelink Ocean Data Assimilation System (BODAS) and the Ocean Forecasting Australia Model (OFAM) grid, which are used in Australia's operational ocean forecast system (Brassington et al. 2007). A description of BODAS and OFAM is provided by Oke et al. (2005, 2008). Results from a series of observing system experiments using this system are presented by Oke and Schiller (2007), and analysis of the circulation around Australia from a 15-yr reanalysis are presented by Schiller et al. (2008).

We do not seek to present a comprehensive assessment of the sensitivity of an ocean forecast system to different RE estimates. Such an assessment is complicated by issues such as initialization. Rather, we seek to demonstrate some of the impacts that different estimates of RE can have on analyses for a realistic ocean forecast system. One of the unique aspects of OFAM is its horizontal resolution. OFAM is eddy resolving around Australia, with 1/10° grid spacing, and is coarser elsewhere, with 2° grid spacing in the North Altantic Ocean. This is an example in which we might expect the use of a spatially uniform estimate for RE to be less optimal. To demonstrate this, we present an example of the increments to η in the North Atlantic Ocean, where the resolution is coarse, and in the Tasman Sea, where the model has a high resolution.

We consider the case in which atSLA observations from altimetry are assimilated. Typically, for this type of application, where the spatial resolution of the observations (i.e., approximately 7 km for atSLA) is finer than the grid resolution (i.e., 0.1°–2°), it is common to compute superobservations (e.g., Ducet et al. 2000; Cummings 2005; Oke et al. 2008). We note that the process of computing superobservations eliminates much of the RE. However, there are many cases when it is not possible to compute superobservations because of the spatial sparsity of the data; for example, in situ observations are assimilated from profiling floats or moorings. We attempt to represent these common scenarios by simply subsampling the altimeter observations, so that fewer observations are directly assimilated in the coarse-resolution region relative to the high-resolution region. Specifically, we limit the density of observations to be no greater than one observation for every 0.5° × 0.5° around Australia and for every 2° × 2° in the North Atlantic. The observations therefore contain a sampling error that should be reflected in their RE estimates. The examples in the North Atlantic are intended to represent the assimilation of observations from a sparse observing network; the examples in the Tasman Sea are intended to represent the assimilation of observations from a dense observation network.

We present results from three cases. Two cases use a

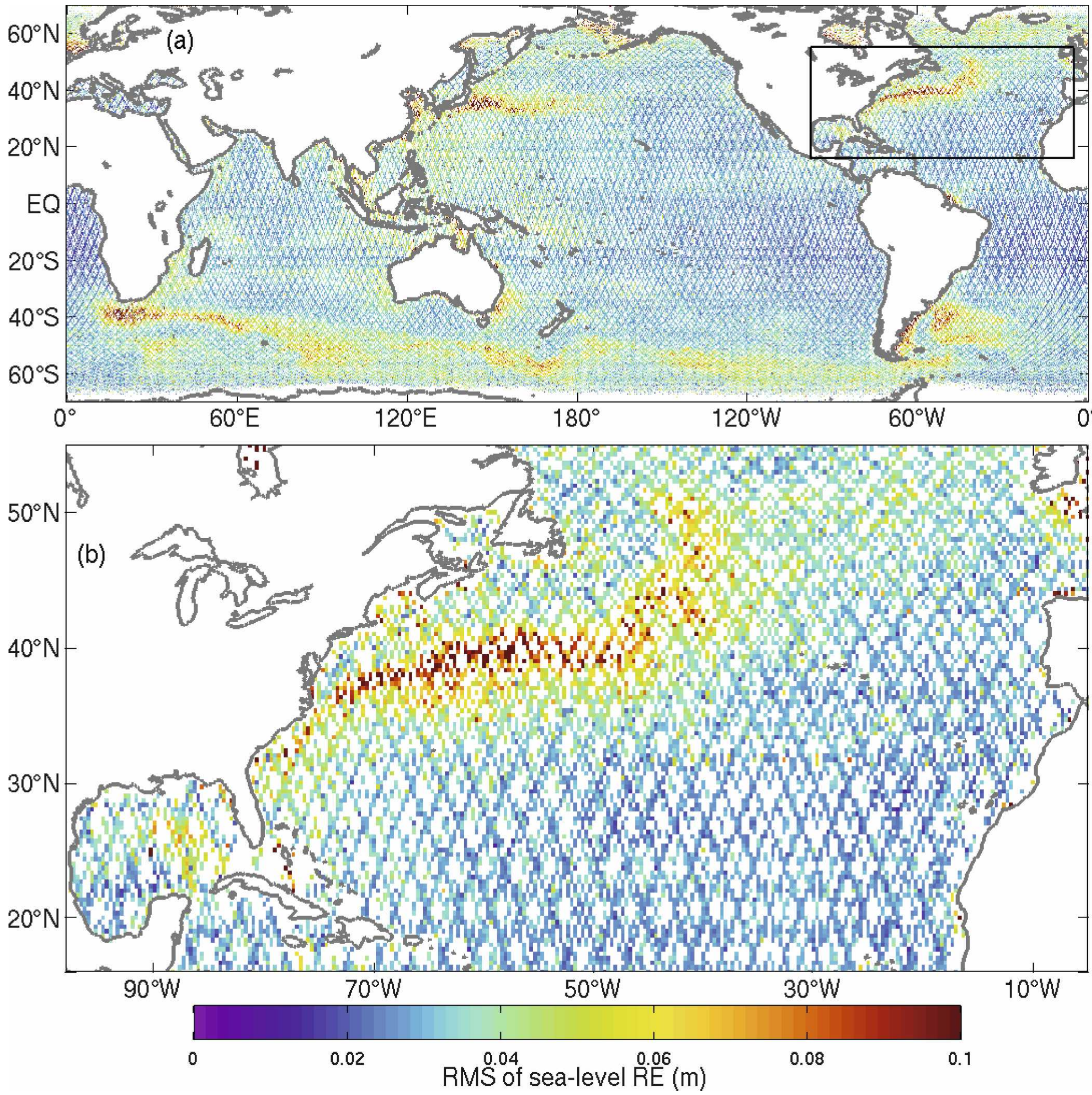

FIG. 7. RMS of the RE for η using the atSLA-based method for a 1/3° global grid: (a) the entire globe and (b) the North Atlantic Ocean.

spatially uniform estimate for RE—one with arbitrarily small RE (RE = 0 m) and one with arbitrarily large RE (RE = 0.1 m). The third case uses spatially varying RE estimates derived from atSLA observations as described in section 2. Figure 8 shows examples of increments for η in the North Atlantic Ocean, where OFAM has a 2° resolution, and in the Tasman Sea, where OFAM has a 1/10° resolution.

The observations in the North Atlantic show a somewhat random scattering of positive and negative anomalies to η (Fig. 8a). This is what we expect for a random sample of a field with energetic mesoscale variability. The increments to η in the North Atlantic, where the grid resolution is 2°, show some similar features for all cases. However, it is clear that for the case with RE = 0 m, the observations are overfitted, with several large-magnitude features generated from only one or two observations (e.g., Fig. 8c; 40°N, 65°W; or 35°N, 75°W). By contrast, the increments to η in the case using the atSLA-derived RE estimates are quite smooth, with only relatively broadscale features evident in the North Atlantic (Fig. 8e). More extreme is the case with RE = 0.1 m, showing η increments with similar features to that of the atSLA-derived case but with smaller magnitudes (Fig. 8g).

The observations in the Tasman Sea show a series of

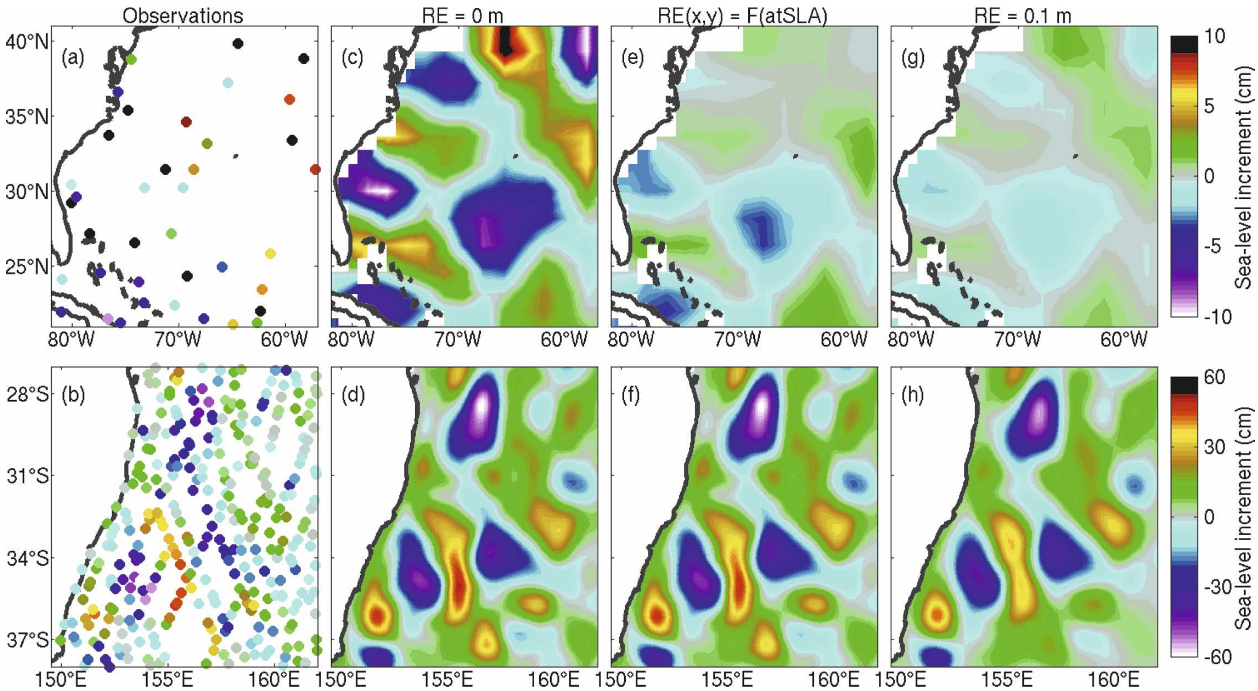

FIG. 8. An example of increments to η for OFAM in the (top) North Atlantic Ocean and the (bottom) Tasman Sea, where the horizontal grid spacing is 2° and 0.1°, respectively. (a), (b) The locations are values of the observations and η increments for the case, where (c), (d) RE is spatially uniform and small (zero), (e), (f) RE is spatially varying according to the atSLA data, and (g), (h) RE is spatially uniform and large (0.1 m).

spatially coherent positive and negative anomalies to η (Fig. 8b). The increments to η in the Tasman Sea, where the resolution is 1/10°, show very similar features for all cases. There is no significant difference between the η increments for the case with RE = 0 m and the case with atSLA-derived RE, with both cases showing close agreement with observations (Figs. 8b,d,f). By contrast, for the case using RE = 0.1 m, the magnitude of the mesoscale features is smaller and some small-scale features are barely evident in the map of η increments (e.g., Fig. 8h; 38°S, 157°E).

The results shown in Fig. 8 draw us to the general conclusion that the case using arbitrarily small RE leads to overfitted observations in the coarse-resolution region; that is, we appear to be fitting noise. By contrast, Fig. 8 suggests that the case using arbitrarily large RE leads to underfitted observations in all regions; that is, we appear to be discarding some useful information. By contrast, the case using spatially varying estimates of RE lead to analysis increments that do not appear to grossly underfit or grossly overfit the observations anywhere. Although this type of comparison does not validate the atSLA-derived RE estimates in a quantitative sense, the results support the contention that misspecified RE can lead to a suboptimal data assimilation and that our spatially varying estimates appear to produce reasonable results everywhere.

4. Discussion

There are some obvious limitations of both the mSLA-based method and the atSLA-based method outlined above. As a result, neither method should be expected to provide estimates for RE that are completely reliable. However, because we expect the mSLA-based method to underestimate the RE and the atSLA-based method to overestimate the RE, we also expect that the appropriate RE for data assimilation purposes lies somewhere between these two estimates. We argue that in the absence of a better approach, these methods could be used for ocean data assimilation studies and perhaps tuned through trial assimilation simulations using consistency checks (e.g., chi-squared test) and through analysis of other statistical properties of the assimilation (e.g., rank histograms).

A significant advantage of the methods described above is that they give inhomogeneous and spatially resolved estimates of the RE. Consequently, this approach should give more precise estimates of the observation error covariance $\mathbf{R}$ than other estimates currently in use (see section 1). This potentially yields a more optimal data assimilation.

Both methods described above provide an ensemble of RE estimates. In theory, these could be used to estimate the spatiotemporal correlations of RE to calculate the off-diagonal elements of **R**. However, the nature of the above-described methods makes this somewhat inappropriate. Specifically, although the mSLA-derived estimates may provide the spatial resolution needed to estimate these fields (i.e., 1/3° resolution), the spatial correlations strongly depend on the length scales used during the OI mapping procedure. By contrast, the atSLA-derived estimates do not depend on any mapping length scales, but they only yield grid-cell averages for the RE. Consequently, we have not undertaken a significant effort to extract information about the off-diagonal elements of **R** in this study. This area of data assimilation requires some attention.

Clearly, we propose these methods with oceanographic applications in mind. In particular, we argue that RE estimates of η can be obtained from either mSLA or atSLA observations that are freely available and widely used. Also, composite maps of satellite-derived SST could be used to estimate the RE for SST. We also note that this method can be easily adapted to three dimensions for applications in which suitable three-dimensional gridded fields are available.

The trend in operational ocean models is toward higher horizontal resolution. As an example, Mercator runs a suite of operational ocean forecast systems ranging from 1/15° in the North Atlantic Ocean to 1/4° for the whole globe (Brasseur et al. 2006); the Naval Research Laboratories (NRL) runs a 1/12°-resolution global model (Barron et al. 2006); and Bluelink runs a model with a 1/10° resolution around Australia (Oke et al. 2005, 2008; Brassington et al. 2007). Clearly, RE decreases as the resolution of the model improves.

There are some observing platforms that have a footprint that is coarser than the model resolution. Examples include 25-km microwave SST retrievals or 7-km along-track altimeter data. Provided such observations represent some average of the region of the swath or track, the model should be averaged to match the footprint of the observations, and thus there would be no RE because of limitations of model resolution. In that case, the main source of observation error would be measurement error.

5. Conclusions

This paper describes two simple and efficient methods for calculating consistent estimates of the RE for η, T, and S observations. Such estimates are required for any data assimilation system. We argue that RE is a function of the model resolution and has subgrid-scale features. For coarse-resolution applications, estimates of the RE, including the subgrid-scale features, can be obtained using the proposed mSLA-based method. For applications to intermediate, eddy-permitting, and even eddy-resolving models, the proposed atSLA-based method may prove beneficial.

We suggest that mSLA, satellite SST, or raw along-track altimetry can be used to estimate the RE for oceanic observations. Although this study has been motivated by data assimilation, the error estimates are arguably more widely applicable; for example, any undertaking to compare output from a model and observations could use RE estimates to assess whether the agreement between the modeled and observed fields are within expected error bars.

Our calculations indicate that there is significant spatial variability in the RE for η, T, and S. This implies that the use of homogeneous observation error variance estimates for ocean data assimilation is likely to be suboptimal. We argue that our simple method is a step toward more accurate estimates of the observation error variance, and therefore a step toward more optimal data assimilation.

Acknowledgments. This research is funded by Australia's CSIRO through appropriation funding and by the U.S. Office of Naval Research Ocean Modeling Program through Grants N000140410345 and N000140711054. The altimeter products were produced by Ssalto/Duacs and distributed by AVISO, with support from CNES.

REFERENCES

Anderson, J. L., B. Wyman, S. Zhang, and T. Hoar, 2005: Assimilation of surface pressure observations using an ensemble filter in an idealized global atmospheric prediction system. *J. Atmos. Sci.,* **62,** 2921–2938.

Barron, C. N., A. B. Kara, P. J. Martin, R. C. Rhodes, and L. F. Smedstad, 2006: Formulation, implementation and examination of vertical coordinate choices in the Global Navy Coastal Ocean Model (NCOM). *Ocean Modell.,* **11,** 347–375.

Bishop, C. H., B. J. Etherton, and S. J. Majumdar, 2001: Adaptive sampling with the ensemble transform Kalman filter. Part I: Theoretical aspects. *Mon. Wea. Rev.,* **129,** 420–436.

Brasseur, P., and Coauthors, 2005: Data assimilation for marine monitoring and prediction: The MERCATOR operational systems and the MERSEA developments. *Quart. J. Roy. Meteor. Soc.,* **131,** 3561–3582.

Brassington, G. B., T. Pugh, C. Spillman, E. Schulz, H. Beggs, A. Schiller, and P. R. Oke, 2007: BLUElink: Development of operational oceanography and servicing in Australia. *J. Res. Pract. Inf. Tech.,* **39,** 151–164.

Cooper, M., and K. Haines, 1996: Altimetric assimilation with water property conservation. *J. Geophys. Res.,* **101,** 1059–1077.

Cummings, J. A., 2005: Operational multivariate ocean data assimilation. *Quart. J. Roy. Meteor. Soc.,* **131,** 3583–3604.

Daley, R., 1992: Estimating model-error covariances for application to atmospheric data assimilation. *Mon. Wea. Rev.,* **120,** 1735–1746.

——, 1993: Estimating observation error statistics for atmospheric data assimilation. *Ann. Geophys. Atmos. Hydro. Space Sci.,* **11,** 634–647.

Derber, J., and A. Rosati, 1989: A global oceanic data assimilation system. *J. Phys. Oceanogr.,* **19,** 1333–1347.

Desroziers, G., A. Brachemi, and B. Hamadache, 2001: Estimation of the representativeness error caused by the incremental formulation of variational data assimilation. *Quart. J. Roy. Meteor. Soc.,* **127,** 1775–1794.

Ducet, N., P.-Y. Le Traon, and G. Reverdin, 2000: Global high-resolution mapping of ocean circulation from TOPEX/Poseidon and ERS-1 and -2. *J. Geophys. Res.,* **105,** 19 477–19 498.

Etherton, B. J., and C. H. Bishop, 2004: Resilience of hybrid ensemble/3DVAR analysis schemes to model error and ensemble covariance error. *Mon. Wea. Rev.,* **132,** 1065–1080.

Evensen, G., 2003: The ensemble Kalman filter: Theoretical formulation and practical implementation. *Ocean Dyn.,* **53,** 343–367.

Fox, A. D., K. Haines, B. A. deCuevas, and D. J. Webb, 2000: Altimeter assimilation in the OCCAM global model. Part I: A twin experiment. *J. Mar. Syst.,* **26,** 303–322.

Houtekamer, P. L., and H. L. Mitchell, 2005: Ensemble Kalman filtering. *Quart. J. Roy. Meteor. Soc.,* **131,** 3269–3289.

Janic, T., and S. E. Cohn, 2006: Treatment of observation error due to unresolved scales in atmospheric data assimilation. *Mon. Wea. Rev.,* **134,** 2900–2915.

Kohl, A., D. Dommenget, K. Ueyoshi, and D. Stammer, 2007: The global ECCO 1952–2001 ocean synthesis. The ECCO Rep. Series 40, 43 pp.

Leeuwenburgh, O., 2007: Validation of an EnKF system for OGCM initialization assimilating temperature, salinity, and surface height measurements. *Mon. Wea. Rev.,* **135,** 125–139.

Levitus, S., and T. P Boyer, 1994: *Temperature.* Vol. 4, *World Ocean Atlas 1994,* NOAA Atlas NESDIS 4, 117 pp.

Liu, Z.-Q., and F. Rabier, 2002: The interaction between model resolution, observation resolution and observation density in data assimilation: A one-dimensional study. *Quart. J. Roy. Meteor. Soc.,* **128,** 1367–1386.

Lorenc, A. C., 1986: Analysis methods for numerical weather prediction. *Quart. J. Roy. Meteor. Soc.,* **112,** 1177–1194.

Mitchell, H. L., and R. Daley, 1997: Discretization error and signal/error correlation in atmospheric data assimilation. *Tellus,* **49A,** 54–73.

——, and P. L. Houtekamer, 2000: An adaptive ensemble Kalman filter. *Mon. Wea. Rev.,* **128,** 416–433.

Ngodock, H. E., G. A. Jacobs, and M. Chen, 2006: The representer method, the ensemble Kalman filter and the ensemble Kalman smoother: A comparison study using a nonlinear reduced gravity ocean model. *Ocean Modell.,* **12,** 378–400.

Oke, P. R., and A. Schiller, 2007: Impact of Argo, SST, and altimeter data on an eddy-resolving ocean reanalysis. *Geophys. Res. Lett.,* **34,** L19601, doi:10.1029/2007GL031549.

——, ——, D. A. Griffin, and G. B. Brassington, 2005: Ensemble data assimilation for an eddy-resolving ocean model of the Australian Region. *Quart. J. Roy. Meteor. Soc.,* **131,** 3301–3311.

——, G. B. Brassington, D. A. Griffin, and A. Schiller, 2008: The Bluelink Ocean Data Assimilation System (BODAS). *Ocean Modell.,* **21,** 46–70.

Pascual, A., Y. Faugère, G. Larnicol, and P.-Y. Le Traon, 2006: Improved description of the ocean mesoscale variability by combining four satellite altimeters. *Geophys. Res. Lett.,* **33,** L02611, doi:10.1029/2005GL024633.

Perez-Brunius, P., T. Rossby, and D. R. Watts, 2004: A method for obtaining the mean transports of ocean currents by combining isopycnal float data with historical hydrography. *J. Atmos. Oceanic Technol.,* **21,** 298–316.

Ponte, R. M., C. Wunsch, and D. Stammer, 2007: Spatial mapping of time-variable errors in *Jason-1* and TOPEX/Poseidon sea surface height measurements. *J. Atmos. Oceanic Technol.,* **24,** 1078–1085.

Richman, J. G., R. N. Miller, and Y. H. Spitz, 2005: Error estimates for assimilation of satellite sea surface temperature data into ocean climate models. *Geophys. Res. Lett.,* **32,** L18608, doi:10.1029/2005GL023591.

Ridgway, K. R., J. R. Dunn, and J. L. Wilkin, 2002: Ocean interpolation by four-dimensional weighted least squares—Application to the waters around Australasia. *J. Atmos. Oceanic Technol.,* **19,** 1357–1375.

Rogel, P., A. T. Weaver, N. Daget, S. Ricci, and E. Machu, 2005: Ensembles of global ocean analyses for seasonal prediction: Impact of temperature assimilation. *Tellus,* **57A,** 375–386.

Schiller, A., P. R. Oke, G. B. Brassington, M. Entel, R. Fiedler, D. A. Griffin, and J. V. Mansbridge, 2008: Eddy-resolving ocean circulation in the Asian-Australian region inferred from an ocean reanalysis effort. *Prog. Oceanogr.,* **76,** 334–365.

Stammer, D., and Coauthors, 2002: Global ocean circulation during 1992–1997, estimated from ocean observations and a general circulation model. *J. Geophys. Res.,* **107,** 3118, doi:10.1029/2001JC000888.

Thacker, W. C., 2003: Data-model-error compatibility. *Ocean Modell.,* **5,** 233–247.

Troccoli, A., and K. Haines, 1999: Use of the temperature–salinity relation in a data assimilation context. *J. Atmos. Oceanic Technol.,* **16,** 2011–2025.

Zaron, E. D., and G. D. Egbert, 2006: Estimating open-ocean barotropic tidal dissipation: The Hawaiian Ridge. *J. Phys. Oceanogr.,* **36,** 1019–1035.